HEFAT2014
10th International Conference on Heat Transfer, Fluid Mechanics and Thermodynamics
14 – 26 July 2014
Orlando, Florida

TRI-THERMAL DEVICE SIZING FOR THERMOPHORESIS DEPOSITION MEASUREMENTS OF NANOPARTICLE SOOT AGGREGATES

Ait Ali Yahia L.[1]*, Gehin.E[2]. and Sagot.B[1]
*Author for correspondence
[1] École Supérieure des Techniques Aéronautiques et Construction Automobile (ESTACA), 34-36 Rue Victor Hugo-92300 Levallois-Perret
[2] Université de Paris Est, 61 Avenue du Général de Gaulle, 94000 Créteil France.
E-mail: lyes.aitaliyahia@estaca.fr

ABSTRACT

Thermophoresis is the motion of particles from the hot to the cold region of a gas subjected to a thermal gradient. This phenomenon contributes to the fouling of EGR (Exhaust Gas Recycling) systems in automotive applications. The aim of this work is to develop a tri thermal device to study the collect of soot particles by thermophoresis. In this device soot particles flow in the annular space between two concentric tubes with imposed temperatures. We will use the so called penetration method which is based on the measurement of particle deposition in the test section. The precision of this method is often limited by the low deposition rates; the main objective of this study is then to size an efficient and compact device for thermophoretic deposition, while respecting mechanical and thermal constraints. We used CFD (Computational Fluid Dynamic) numerical simulations and model results to choose an optimal design of the device, which is composed of hot and cold tubes with diameter respectively equal to 87 and 85mm and with 0.5 meter long tubes.

INTRODUCTION

When a particle is suspended in a gas subjected to a thermal gradient, this particle migrates from the hot to the cold region of the gas. This phenomenon is called thermophoresis, and the moving particles will also experience a drag force. The balance of the thermophoretic and drag forces results in an equilibrium velocity, the expression of this thermophoretic velocity is described as:

$$v_{th} = -K_{th}\frac{\mu_g}{\rho_g}\frac{\nabla T}{T_g} \qquad (1)$$

Several studies concerning the determination of the thermophoretic coefficient K_{th} for spherical particles can be found in the literature (Sagot [1]). However there are limited studies treating the case of non-spherical particles. Recently, Messerer & al.[2] and Brugière & al.[3] proposed experimental devices for the determination of the thermophoretic velocity of soot aggregates.

The experimental determination of the thermophoretic coefficient is usually based on one of the following techniques: measurement of forces (Li & Davis [4], Zheng & Davis [5]), thermophoretic velocities (Prodi & al. [6], [7], Toda & al. [8]), particles selection (Brugière & al.[3]), or deposition efficiencies (Stratmann & Fissan [9], Montassier & al. [10], Romay & al. [11]). For the first technique, it is necessary to determine the drag force, which is very difficult to obtain with non-spherical particles such as soot aggregates. For that reason we chose the so called penetration method, where the deposition rate on a cold wall is obtained by measurement of the particles concentrations upstream and downstream of the test section. Together with a thermophoretic deposition model, those measurements allow the experimental determination of the thermophoretic coefficient K_{th}. The precision of this method is often limited by the low particle deposition rates, which is due to the reduction of the gas to wall temperature difference along the cold wall pipe flow. To overcome this problem, a tri thermal (3*T*) device has been proposed by Sagot & al. [12], where particles flows through an annular space between two concentric tubes with imposed temperatures, where the inner tube is cooled and the outer tube heated.

The aim of this work is then to size an efficient tri thermal device for thermophoretic deposition: the efficiency increases with the thermal gradient, and also by reducing the Reynolds number *Re*. However, a compromise has to be found, as convective effects will appear for high values of Gr/Re^2, *Gr* the Grashof number. We also have to ensure the temperature uniformity along the test section. For that purpose, we will use a CFD numerical simulation to analyze the thermal and velocity profiles, to evaluate the convective effects intensity, and also to determine the hydrodynamic entrance lengths. We will also use an analytical model for the evaluation of the deposition efficiency with a laminar flow and imposed temperatures.

NOMENCLATURE

C	[kg.m^{-3}]	Particle mass concentration
D	[m]	Diameter
e	[m]	Gap
Gr	[-]	Grashof number
J_m	[kg.m^{-2}.s^{-1}]	Thermophoretic mass flux to the cold wall
K_{th}	[-]	Thermophoretic coefficient
L	[m]	Length
L_c	[m]	Length scale for the Grashof number evaluation
L_h	[m]	Hydrodynamic entrance length
$\dot{m}_g$	[kg.s^{-1}]	Gas mass flow-rate
Q_v	[m^3.s^{-1}]	Gas volumetric flow-rate
r	[m]	Radius
T	[K]	Temperature
V	[m.s^{-1}]	Velocity
v_{th}	[m.s^{-1}]	Thermophoretic velocity
z	[m]	Axial coordinate

Special characters

β	[K^{-1}]	Air thermal expansion coefficient
η	[-]	Deposition efficiency
μ_g	[kg.m^{-1}. s^{-1}]	Gas dynamic viscosity
ρ_g	[kg.m^{-3}]	Gas density
∇T	[K.m^{-1}]	Temperature gradient

Subscripts

c	Cold
g,c	Gas, cold wall
g,in	Gas inlet
$g,mean$	Gas, mean temperature, $T_{mean}=(T_c+T_h)/2$
g,h	Gas, hot wall
h	Hot
min	Minimum
max	Maximum
Th	Thermophoretic

SIZING OF THE THERMOPHORETIC DEPOSITION DEVICE

In order to determine the temperature gradient which produces thermophoresis in turbulent flows (Romay & al. [10]; Sagot & al. [11]), it is necessary to use a Nusselt number correlation. Then, by equating the conductive and convective heat flux densities in the boundary layer, an evaluation of the thermal gradient at the wall is obtained. This introduction of a model in an experimental determination might introduce approximation in these measurements. For that reason, we chose a laminar flow configuration for our thermophoretic precipitator, where the temperature gradients can be obtained by analytical resolution of Navier-Stokes and energy equations. However, convective effects might occur while using a laminar flow and those effects have to be evaluated for the tri thermal device. Computational Fluid Dynamic (CFD) has been used for this analysis, where the variations of the gas density with the temperature are taken into account. We also chose a vertical flow (figure 1) in order to avoid tubes bending, and also to eliminate particles deposition by sedimentation.

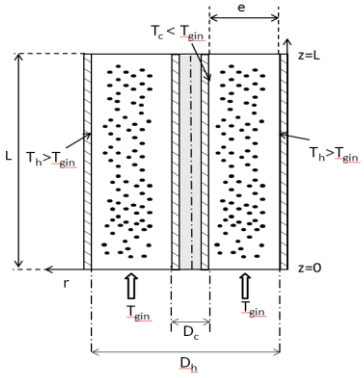

Figure 1 Thermophoretic precipitator (3T).

In a tri thermal device, the gas is cooled by convective transfer to the cold wall (Diameter D_c) and simultaneously heated by the external hot wall (D_h). An equilibrium temperature is thus obtained. In the experimental conditions, the inlet gas temperature will be adjusted to be equal to this bulk temperature, to ensure a uniformity of the gas temperature and temperature gradient.

To determine the particle deposition rate, we express the mass balance over a tube section taking into account the particle deposition flux. We obtain the 1D equation for the axial dependence of the particle masse concentration $C(z)$ for a given particle size:

$$-Q_v \frac{dC}{dz} = J_m(z)\pi D_c \qquad (2)$$

$J_m(z)$: the local mass flux to the cold wall, by thermophoretic effect :

$$J_m(z) = -C(z)\frac{\mu_g}{\rho_g} K_{th} \frac{\frac{dT}{dr}(z, D_c/2)}{T_c} \qquad (3)$$

The thermophoretic velocity in equation (1) is expressed as a function of the local temperature T_g, which is evaluated here at the cold wall temperature. This also applies for the gas properties μ_g and ρ_g. The temperature gradient $\nabla T_c = dT/dr$ being negative to the wall, $J_m(z)$ is then considered positive, and equation (2) becomes :

$$-Q_v \frac{dC}{dz} = -C(z)\frac{\mu_{gc}}{\rho_{gc}} K_{th} \frac{\nabla T_c}{T_c} \pi D_c \qquad (4)$$

In our 3T device, the flow is established and the gas temperature is constant on a streamline, the term $\nabla T_c/T_c$ can thus be considered as constant, after the entry length that will be evaluated. Then we can integrate directly the equation (4) between z=0 to z, in order to obtain the expression of the axial particles mass concentration $C(z)$. With the inlet concentration being noted $C(0)= C_0$, we obtain :

$$C(z) = C_0 \exp\left[\frac{\mu_{g,c}}{\rho_{g,c}\, Q_v} K_{th} \frac{\nabla T_c}{T_c} \pi D_c z\right] \quad (5)$$

The deposition efficiency of particles by thermophoresis within a test section is defined as:

$$\eta_{th}(d_p) = 1 - \frac{C_L}{C_0} \quad (6)$$

The global efficiency can then be written:

$$\eta_{th}(d_p) = 1 - exp\left[\frac{\rho_{g,mean}\, \mu_{g,c}}{\rho_{g,c}\, \dot{m}} K_{th} \frac{\nabla T_c}{T_c} \pi D_c L\right] \quad (7)$$

With $\rho_{g,mean}$ being evaluated at the mean temperature $T_{mean}=(T_c+T_h)/2$. It should be noted that in the exponential, the temperature gradient at the wall ∇T_c is negative.

The results presented in figure 2 are obtained by applying the thermophoretic deposition model (7) with D_c= 85mm, e= 1.5mm, T_c= 278 K, T_h varying from 298 to 508K and Re= 77. For this study we chose K_{th}= 0.5, this value is similar to that obtained by Brugière & al. [2] for soot aggregates. Figure 2 presents the influence of tubes length and temperature difference $\Delta T = T_h - T_c$ on the deposition rate, which increases with the length and temperature gradient.

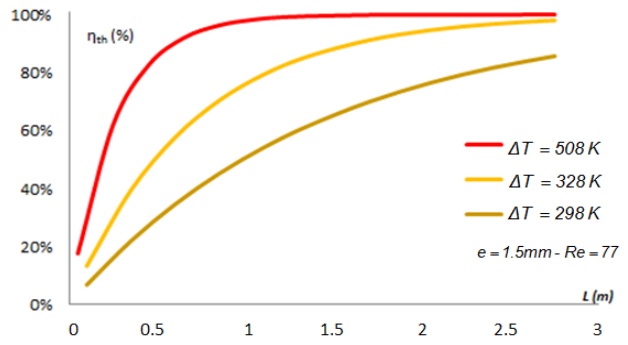

Figure 2 Evolution of the deposition efficiency (eq (6)) with the length L (e= 1.5mm, D_c= 85mm, T_c= 278K, Re= 77 and variable T_h).

CFD NUMERICAL SIMULATION

We conducted a CFD numerical simulation on a 0.5 meter length tri thermal device, with D_c= 85mm, D_h varying from 87 to 91mm, and Reynolds number varying from 62 to 701. T_c , T_h and $T_{g,in}$ are respectively equal to 278 K, 333 K and 305 K. This simulation provided identification of the hydrodynamic entrance length, and also evaluation of the convective effects. An example of a flow subjected to convective effects and an example of established velocity profile are presented in figure 3.

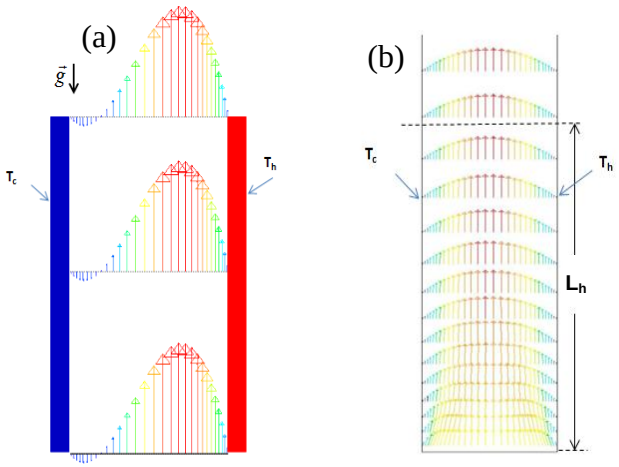

Figure 3 (a) Velocity profiles with convective effects. (b) Establishment of a velocity profile.

As can be seen in figure 3 (a), the convective effects result in a flow acceleration on the hot wall side, and a flow deceleration on the cold wall side, which results in a reversed flow and a strong perturbation of the thermal gradient. According to CFD simulations, the convective effects can be considered negligible when the ratio Gr/Re^2 is lower than 10^{-4}. Gr is the Grashof number given by the relation:

$$Gr = g\beta\Delta T L_c^3 / \nu_{g,mean}^2 \quad (8)$$

Where β is the air thermal expansion coefficient and $\nu_{g,mean}$ the cinematic velocity evaluated at the mean gas temperature. For an annular flow configuration, the reference length L_c is evaluated by the relation (Incropera [13]) :

$$L_c = 2[ln(D_h/D_c)]^{4/3} / [(D_h/2)^{-3/5} + (D_c/2)^{-3/5}]^{5/3} \quad (9)$$

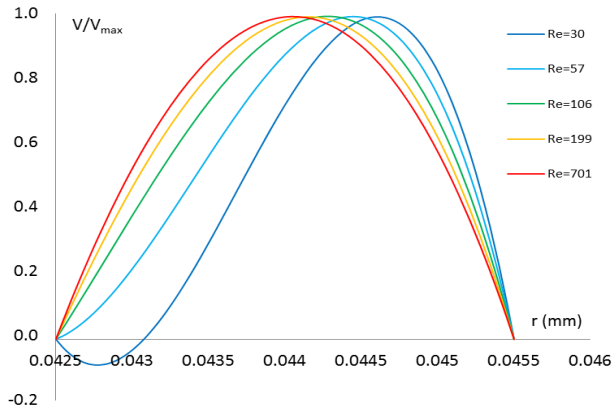

Figure 4 Evolution of the axial velocity with the Reynolds number for e= 3mm.

The results of the CFD simulation are reported in the table 1. It can be seen that the ratio Gr/Re^2 increases with the increase of the gap "e". Thereby for an iso value of the

Reynolds number (Re= 62), it can be seen that between the two cases e= 1mm and e= 3mm, we have a ratio of 100 for the parameter Gr/Re^2, which is due to the strong dependence of the Grashof number on the length L_c^3.

Table 1: Comparative table between the different geometries used in the CFD simulation, with T_h= 333K and T_c= 278 K

D_c (mm)	e (mm)	L_c/e	Re	L_h/L	Gr/Re^2
85	1	0.18	62 - 679	0.4 -7%	$9.19\ 10^{-5} – 7.55\ 10^{-6}$
85	1.25	0.19	62 - 572	1 – 6%	$2.21\ 10^{-4} – 2.59\ 10^{-6}$
85	1.5	0.20	62 - 570	1.4 – 10%	$4.56\ 10^{-4} – 5.39\ 10^{-6}$
85	2	0.22	62 - 586	(-)* - 12%	$1.43\ 10^{-3} – 1.63\ 10^{-5}$
85	3	0.25	62 - 701	(-)* - 20%	$7.17\ 10^{-3} – 5.60\ 10^{-5}$

(*) velocity profiles are not established for low values of Reynolds number

An increase of the gap size causes the apparition of convective effects; those effects subside when increasing the Reynolds number (figure 4). For a gap e= 1mm it can be seen that the longest hydrodynamic entrance length L_h is about 5% of the length L (figure 5), for the highest value of the Reynolds number. The hydrodynamic entrance length increases with the gap size "e" (for e= 3mm and Re= 701: L_h/L= *20%).*

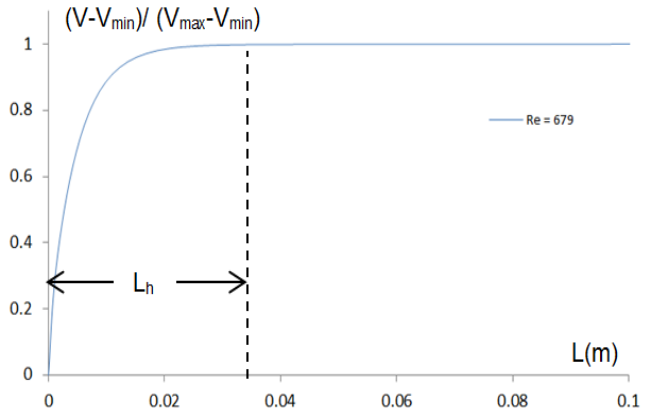

Figure 5 Evolution of the axial velocity with the length.

RESULTS OF THE MODEL

We applied our model (equation (7)) for the same gaps reported in table 1, with L= 0.5m, T_c= 278K, T_h= 333K and with a thermophoretic coefficient K_{th}=0.5. The thermal gradients ∇T_c are obtained by CFD simulation for every mass flow. The results obtained by applying the efficiency model are reported in figure 6.

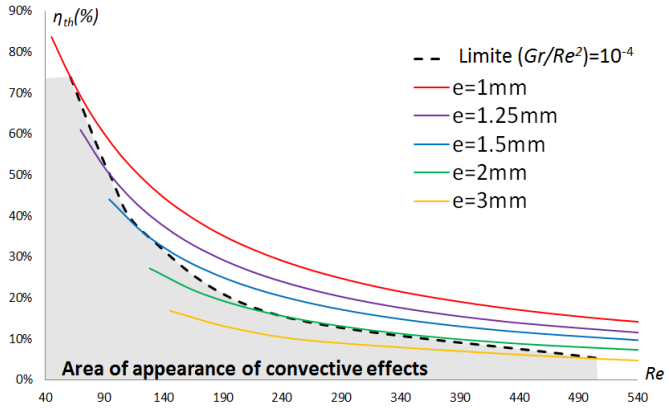

Figure 6 Thermophoretic deposition efficiency

For a given gap size, the deposition efficiency reduces when increasing the Reynolds number. For a fixed value of the Reynolds number, this deposition efficiency decreases when the gap size increases. It can be seen in figure 6 that the critical Reynolds number that corresponds to the apparition of convective effects decreases significantly when reducing the gap "e". This corresponds to an increase of the thermophoretic deposition efficiencies due to higher values of the residence time. We denote that beyond the limit presented by the dashed black line ($Gr/Re^2 < 10^{-4}$), the best deposition rates are obtained with a gap e= 1mm (for Re= 62, the deposition efficiency is about 74%).

It should be noted that the particles deposition rate increases with the length of the deposition area (see figure 2), for fixed values of the temperature gradient and mass flow rate.

For an imposed value of the deposition efficiency η_{th}= 50%, and a fixed value Gr/Re^2= 10^{-4}, we report in figure 7 the evolution of necessary deposition length for this target efficiency, as a function of the gap size e.

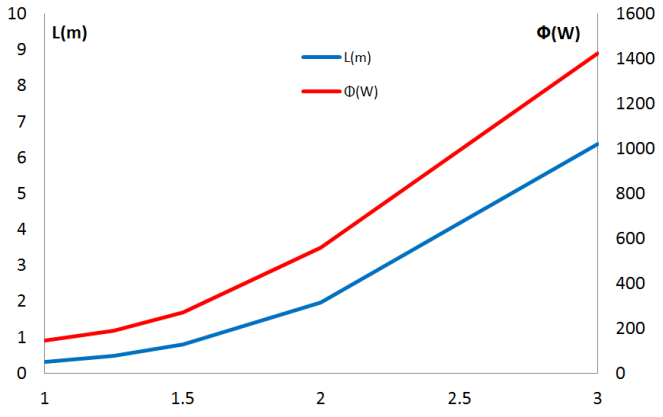

Figure 7 Representative domains used for thermal modelling

We also report in figure 7 the corresponding thermal power transferred at the walls. Indeed those thermal powers (convection+ radiation) should be transferred to the hot wall by a high flow rate circulation of temperature regulated silicon oil,

and extracted from the cold wall side by another temperature regulated loop (use of a cryostat).

As can be seen in figure 7, to reach a deposition efficiency of 50% with e= 3mm and Gr/Re^2= 10^{-4}, a 6.4 meter length is necessary, with a corresponding transferred power of about 1.4kW. It should be noted that to ensure a temperature uniformity along the tubes, the power transferred should be as low as possible. The best compromise can be achieved by a reduction of the gap size together with the device length, while avoiding convective effects and ensuring the best deposition rates. The manufacturing feasibility is then the only limit. With e= 1mm, a 1% tolerance on the gap value corresponds to $10\mu m$ tolerance on the diameter size, that we must ensure over a 0.5 m length. That's a limit that can be achieved, which justify this final arrangement for the design of this new device.

CONCLUSION

A tri-thermal device sizing for thermophoresis deposition measurements is proposed in this study. We built a deposition model with a laminar flow, where temperature gradients are obtained by CFD numerical simulation. The results presented in this study shows that beyond the limit of convective effects appearances (Gr/Re^2 <10^{-4}), the deposition efficiency tends to increase when reducing the gap size. The reduction of the gap size permits to shorten the tubes length for a fixed efficiency, while reducing the thermal powers transferred. It should be noted that in term of mechanical design, it's difficult to have a gap size less than 1 mm, which represent the limit fixed in this study.

The selected configuration is the one which combines:

- Compactness (L= 0.5m).
- Limited power transferred.
- Negligible convective effects ($Gr/Re^2 < 10^{-4}$).
- High deposition rates, which will allow an accurate determination of the experimental thermophoretic coefficient, as a function of soot aggregates morphology parameters.

REFERENCES

[1] B. Sagot, "Thermophoresis for spherical particles," *J. Aerosol Sci.*, vol. 65, pp. 10–20, Nov. 2013.

[2] A. Messerer, R. Niessner, and U. Pöschl, "Thermophoretic deposition of soot aerosol particles under experimental conditions relevant for modern diesel engine exhaust gas systems," *J. Aerosol Sci.*, vol. 34, no. 8, pp. 1009–1021, Aug. 2003.

[3] E. Brugière, F. Gensdarmes, F.-X. Ouf, J. Yon, A. Coppalle, and D. Boulaud, "Design and performance of a new device for the study of thermophoresis: The radial flow thermophoretic analyser," *J. Aerosol Sci.*, vol. 61, pp. 1–12, Jul. 2013.

[4] W. Li and E. James Davis, "Measurement of the thermophoretic force by electrodynamic levitation: Microspheres in air," *J. Aerosol Sci.*, vol. 26, no. 7, pp. 1063–1083, Oct. 1995.

[5] F. Zheng and E. J. Davis, "Thermophoretic force measurements of aggregates of micro-spheres," *J. Aerosol Sci.*, vol. 32, no. 12, pp. 1421–1435, Dec. 2001.

[6] F. Prodi, G. Santachiara, and V. Prodi, "Measurements of thermophoretic velocities of aerosol particles in the transition region," *J. Aerosol Sci.*, vol. 10, no. 4, pp. 421–425, 1979.

[7] F. Prodi, G. Santachiara, and C. Cornetti, "Measurements of diffusiophoretic velocities of aerosol particles in the transition region," *J. Aerosol Sci.*, vol. 33, no. 1, pp. 181–188, Jan. 2002.

[8] A. Toda, Y. Ohi, R. Dobashi, T. Hirano, and T. Sakuraya, "Accurate measurement of thermophoretic effect in microgravity," *J. Chem. Phys.*, vol. 105, no. 16, pp. 7083–7087, Oct. 1996.

[9] F. Stratmann and H. Fissan, "Experimental and theoretical study of submicron particle transport in cooled laminar tube flow due to combined convection, diffusion, and thermophoresis," *J. Aerosol Sci.*, vol. 20, no. 8, pp. 899–902, 1989.

[10] N. Montassier, D. Boulaud, F. Stratmann, and H. Fissan, "Comparison between experimental study and theoretical model of thermophoretic particle deposition in laminar tube flow," *J. Aerosol Sci.*, vol. 21, Supplement 1, pp. S85–S88, 1990.

[11] F. J. Romay, S. S. Takagaki, D. Y. H. Pui, and B. Y. H. Liu, "Thermophoretic deposition of aerosol particles in turbulent pipe flow," *J. Aerosol Sci.*, vol. 29, no. 8, pp. 943–959, Sep. 1998.

[12] B. Sagot, G. Antonini, and F. Buron, "Annular flow configuration with high deposition efficiency for the experimental determination of thermophoretic diffusion coefficients," *J. Aerosol Sci.*, vol. 40, no. 12, pp. 1030–1049, Dec. 2009.

[13] F. P. Incropera, *Fundamentals of heat and mass transfer*. John Wiley, 2007.